Available online at **www.joac.info**

ISSN: 2278-1862

Journal of Applicable Chemistry, 2012, 1 (2):319-329

(International Peer Reviewed Journal)

Study of Ozone Depletion by Halon-2402 in Stratospheric Layer Using Quantum Calculation Methods

Aqeel A-Hussein and Abbas A-Ali Drea*

Chemistry Department, College of Science, Babylon University, Hilla, IRAQ
E-mail: *aadreab@yahoo.com*

ABSTRACT

Structural properties of ozone and Halon-2402(1,2-dibromotetrafluoroethane) have been calculated using quantum methods likes DFT, ab-initio and semi-empirical (implemented in Hyperchem package 8.0) .Examination of bond reactivity for reaction component have been determined according to MP2//6-31G**(p,d) level of theories. Molecular orbital and their energy gap has been calculated using B3LYP//6-31G(d) and B3LYP//3-21++G**(p,d) level and parameter of bonds by ROHF//6-31G**(p,d) level. Values of rate constant and the reaction energy barrier were determine for all free radical reactions using MP2//3-21G**(2spd) level of theory. Steady state approximation method has been used to estimate the rate law of the depletion reaction.

It was found that the energy gap of ozone and Halon-2402 is 90.23 and 163 kCal/mol respectively. Photolysis reaction of Halon-2402 occurs through C-Br bond by 92.3 kCal/mol (309.95 nm)of light energy. The reaction of bromine radical with ozone is spontaneous and exothermic with energy barrier equal to 0.044 kCal/mol and rate constant equal to 3×10^{13} $mol^{-1}dm^3s^{-1}$, A= 2.33×10^{13} at STP. The mechanism of ozone depletion produced alkoxy radical by consuming four moles of ozone.

Keywords: Halone-2402, photolysis, Ozone depletion, Radical, potential energy surface, bond dissociation energy, MP2, B3LYP, and PM3.

INTRODUCTION

Photolysis of molecular oxygen leads to ozone formation, this process absorbed all wavelengths shorter than 200 and 310 nm of sun light radiation but ozone is less stable than oxygen, though this phenomena play an important role for atmosphere protection from harmful

radiations[1-7]. Different pollutants can reach Ozone's layer, that may be due to human uses . Halo-hydrocarbons are the major sources of the most common pollutant agent in the atmosphere. Organic halides act as an important agent in the ozone depletion due their providing of anthropogenic halogen atoms into atmospheric layers [8,9]. Halon-2402(1,2-dibromotetrafluoroethane) is a colorless liquid with a boiling point of 47.2 °C and it is occasionally used in different manner commercially [10] . Halon-2402 has relatively long lifetime in the atmosphere, and they break in the stratosphere to release reactive bromine that causes severely damaging to ozone with 10–100 times more than chlorine [11,12] . Reactions involving bromine are estimated to be responsible for 25 percent of the chemical destruction of ozone over Antarctica and 50 percent over the Arctic [13]. The measurements of the halogenated species in the tropical troop use found that Halon-2402 detected between 30 °S and 30 °N latitudes. Transporting from the troposphere into the stratosphere occurs mainly in this region. Since the concentration of Halon-2402 in tropical use provides a good measure of the relative mixing ratio in the stratosphere. The chemistry of intermediate compounds that are involved by Ozone's reaction with pollutant agents is limited, however laboratory and modeling studies are helping to quantify and reduce some of the uncertainties [14-17] . Great interest of theoretical studies to investigate the mechanisms for these reactions to find them according to most probable suggested mechanism in stratosphere layer [18,19].

In the present work, the quantum calculation methods are using such as HF, DFT and MP2 methods in combination with 6-31G**, 3-21G+(s,sp,6d) and 3-21++G** basis sets for C, F and Br atoms in addition to PM3CI(4x4) to estimate the geometry optimization and single point calculations for Halon-2402 ,ozone and all chemical species that are involved in the suggested depletion mechanism. Calculations of first and second dissociation energy carry out on $C_2F_4Br_2$. Study of the reactions and the suggested transition states through the thermodynamic and kinetic results in vacuum. Suggested reaction mechanism of ozone depletion through Halon-2402, and the rate law estimation by steady-state approximation.

MATERIALS AND METHODS

Calculation Details: All theoretical calculations were performed using computational implemented in the Hyperchem package 8.0.9 [20]. Optimized geometries of Halon-2402 and ozone have been done using the B3LYP of DFT[21-23] and MP2 of Ab-initio[24,25] methods with basis sets are 3-21G* [26-28] and 6-31G**[29-32] , in addition to Restricted open shell Hartree-Fock (ROHF)[33-35] and also PM3CI(4x4) of semi-empirical[36-37] . A single point calculation had been used to give up the static properties of a molecule includes potential energy , electrostatic potential, molecular orbital energies, and the coefficients of molecular orbital's for ground ,or excited states. Vibrational analysis carried out through the same methods to deduced the nature of stationary points with zero point energy and all the stationary points have been identified with imaginary frequency[38] . Potential energy stability had been performed at B3LYP/3-21G+(s,sp,6d)//MP2/3-21G(s,sp,6d) level of theory for length, angle and torsion of bonds in $C_2F_4Br_2$ while at MP2//6-31G**(p,d) level of theory . First and second dissociation reaction for C-Br bonds in $C_2F_4Br_2$ had been studied by HF, MP2 and DFT(B3LYP,B3PW91) combining with 6-31G, 6-31G*, 6-31G**, 4-31G, 4-31G*[39] , 3-21G (s,sp,6d) and 3-21++G** basis sets in addition to PM3CI(4x4) . Geometry optimization of reactants, transition states and products for reaction between $Br^{\bullet}$ and $^{\bullet}C_2F_4Br$ with ozone at PM3CI(4x4) and MP2//3-21G**(2spd) level . Potential energy surface performed by mapping reactants into products in

order to calculate the energy barrier at PM3CI(4x4) and MP2//3-21G**(2spd) level of theory. Semi-empirical calculations at PM3 have been performed to estimate the thermodynamic values at 298.15 K. To ascertain that the identified transition states connect reactant and products smoothly [38]

RESULTS AND DISCUSSION

Structural properties of ozone have been studied using different quantum calculations methods to estimate the chemical reactivity . Table 1 shows the structural properties of ozone ,The symmetry of ozone is C_{2v} measured by all methods[40]. The heat of formation calculated by PM3 equal to 31.4 kCal/mol that's good agreement with the experimental (34.6 kCal/mol). The MP2//3-21G(d) method give up low value of dipole moment equal to 0.107277 D, while same basis set gives 0.38688 D with B3LYP. The high dipole moment value is measured by PM3 follow its B3LYP//6-31G**(p,d) level of theory. There is good agrees between the MP2//6-31G**(p,d) and B3LYP//6-31G(d) level of theory with experimental value (0.5 D) . The O-O bond measured by MP2 method with basis sets 3-21G(d), 6-21G(d) and 6-31G**(p,d) are equal to 1.3893, 1.3002 and 1.3007 Å respectively . Net atomic Mullikan charge calculated by B3LYP//6-31G**(p,d) level give up more negative charge on the oxygen atom O_1 and O_3 equal to -0.129335 and -0.129327 coulomb respectively and more positive charge on O_2 equal to 0.258662 coulomb, come after the B3LYP//6-31G(d) level. While the MP2//3-21G(d) level given less negative charge on O_1 and O_3 equal to -0.044332 and -0.044382 coulomb respectively. The HOMO, LUMO and the lowest energy band gap, and energy excitation equal to90.23 kCal/mol by B3LYP//6-31G(d) level of theory[43].

Table 1. Structural properties of ozone calculated at different quantum methods

Method / Type of calculation		PM3-CI(4x4)	MP2// 3-21G(d)	MP2// 6-31G(d)	MP2// 6-31G** (p, d)	B3LYP// 3-21G(d)	B3LYP// 6-31G(d)	B3LYP// 6-31G** (p,d)
Total energy $\times 10^4$		-2.01644	-14.02302	-14.11077	-141118.1	-14.06007	-14.13878	-14.139604
Dipole moment		0.763	0.107277	0.398041	0.467235	0.386880	0.514609	0.685610
Zero point energy		4.6	7.164847	6.111405	6.131970	3.94896	4.641621	4.5866564
HOMO		-289.41	-296.25	-309.34	-301.3	-187.43	-213.93	-204.13
LUMO		-58.3	-21.55	-37.98	-20.42	-96.4	-123.7	-112.2
E_g		231.11	274.7	272	280.88	91.03	90.23	91.93
Bond length	O_1-O_2	1.255	1.3893	1.3002	1.3007	1.3670	1.2647	1.2636
	O_2-O_3	1.255	1.3893	1.3002	1.3007	1.3669	1.2647	1.2638
Bond angle		114.3	113.4884	116.3031	116.4950	116.029	117.1285	117.1009
Mulliken charges	O_1	-0.282	-0.044332	-0.086532	-0.110148	-0.058445	-0.115568	-0.129335
	O_2	0.563	0.088714	0.172921	0.220287	0.116906	0.231147	0.258662
	O_3	-0.281	-0.044382	-0.086389	-0.110139	-0.058461	-0.115579	-0.129327

Energetic values in kCal/mol, bond length in Å, bond angle in degree, Dipole moment in Debye (D), Mullikan charges in coulomb units.

Structural properties of Halon-2402 had been performed at PM3, Hartree-Fock (ROHF), MP2 and B3LYP. 1,2-dibromotetrafluoroethane is a weak polar molecule as shown in table 2. The zero point energy is 14.59 kCal/mol calculated by B3LYP//3-21++G**(p,d) level. Frontal Molecular Orbital's the HOMO and LUMO results are given in table 2. The B3LYP//3-

21++G**(p,d) given lowest energy band gap equal to 163.7 kCal/mol therefore any excitation process occurrence will be needed to 163.7 kCal/mol of energy[44] . The calculated atomic charge for bromine atom by all method have positive excess charge except B3LYP,MP2//3-21+G(s,sp,6d) level is negative excess charge while at same time fluorine atom have negative excess charge with all methods, subsequently, the C-Br bond is more chemical reactivity than C-F bond[45] .

Table 2. Energetic properties of $C_2F_4Br_2$ calculated at different quantum methods

Method / Energy Calculation		PM3-microstate CI(4x4)	ROHF// 6-31G**	MP2// 6-31G** (p,d)	B3LYP, MP2 // 3-21G+ (s,sp,6d)	B3LYP// 3-21++G** (p,d)	B3LYP// 6-31G** (p,d
Total energy $\times 10^5$		-0.624088	-35.224133	-35.236292	-34.90277	-35.12026	-35.257115
Dipole moment		0.0002	0.0001	0.0001	0.0002	0.000102	0.000104
Zero point energy		17.03	17.001	15.7	15.212	14.95	15.284
HOMO		-277.411	-260.33	-244.5	-115.531	-183.4	-110.55
LUMO		-53.176	-60.4	-47.47	70.794	-19.7	64.35
Δ_g		224.235	199.93	197.03	186.325	163.7	175.05
Mullikan charges	C_1	0.16307	0.267547	0.209310	0.180457	0.305404	0.191112
	C_2	0.16307	0.267547	0.209313	0.180553	0.305350	0.191096
	Br_3	0.009109	0.030108	0. 039693	-0.020653	0.205613	0.016529
	Br_4	0.009109	0.030108	0.039699	-0.020678	0.205641	0.016527
	F_5	-0.08608	-0.148787	-0.124541	-0.079961	-0.255517	-0.103911
	F_6	-0.0861	-0.148867	-0.124459	-0.079889	-0.255481	-0.103721
	F_7	-0.08608	-0.148787	-0.124556	-0.079905	-0.255514	-0.103911
	F_8	-0.0861	-0.148867	-0.124461	-0.079922	-0.255495	-0.103720

Energetic values in kCal/mol, Dipole moment in Debye (D) and Mullikan charges in coulomb

There are two bonds in $C_2F_4Br_2$ molecule ,since the length of C-Br bonds with 1.9211 Å according to ROHF//6-31G**(p,d) and MP2//6-31G**(p,d) level of theory but the length of C-C bond is 1.5441 Å . The C-F bond has 1.3363 Å according to B3LYP,MP2//3-21G(s,sp,6d) level of theory. According to calculations, the C-Br bond is more reactive toward the dissociation process due to lowest stability and its required lowest energy to scission into two free radicals $Br^{\bullet}$ and $^{\bullet}C_2F_4Br$ than C-C and C-F bond[46] . There are four types of bond angles ,as F-C-C, Br-C-C, F-C-F and Br-C-F. They found F-C-C angle equal to 109.2º and 109.2010º calculated by ROHF//6-31G**(p,d) and MP2//6-31G**(p,d) method respectively[47] as shown in table .3 . The ROHF//6-31G**(p,d) and MP2//6-31G**(p,d) method given up 110.6259º and 110.626º respectively for Br-C-C angle . The F-C-F angle is 108.8178º and 108.818º by ROHF//6-31G**(p,d) and MP2//6-31G**(p,d) method. The calculated Br-C-F angle is equal to 109.48º according to ROHF//6-31G**(p,d) and MP2//6-31G**(p,d) method. The torsion angle of Br-C_1-C_2-Br is 180.00º (fixed) calculated by B3LYP, MP2//3-21G+(s, sp,6d) method.

Table 3 Bonds parameters of $C_2F_4Br_2$ calculated at different calculation methods (bond length in Å and bond torsion angle in degree)

Method / Bond	PM3-microstate CI(4x4)	ROHF// 6-31G** (p,d)	MP2// 6-31G** (p,d)	B3LYP, MP2// 3-21G+ (s,sp,6d)	B3LYP// 3-21++G** (p,d)	B3LYP// 6-31G** (p,d)
C_1-Br_3	1.9390	**1.9211**	**1.9211**	1.9393	1.8893	1.9306
C_2-Br_4	1.9392	1.9211	1.9211	1.9393	1.8893	1.9305
C_1-C_2	1.55373	1.535	1.5348	1.5536	**1.5441**	1.5395
C_1-F_5	1.3366	1.3166	1.3166	1.3363	1.4134	1.3462
C_1-F_6	1.3368	1.3166	1.3166	**1.3363**	1.4134	1.3463
C_2-F_7	1.3361	1.3166	1.3166	1.3363	1.4134	1.3463
C_2-F_8	1.3366	1.3166	1.3166	1.3363	1.4134	1.3462
F_8-C_2-F_7	106.3305	**108.8178**	108.818	106.302	106.8401	109.1157
F_8-C_2-Br_4	112.4243	**109.4825**	109.482	112.484	110.4296	109.6092
F_8-C_2-C_1	112.2887	**109.2**	**109.201**	112.26	107.4420	109.0668
F_7-C_2-Br_4	112.4369	**109.4836**	109.484	112.483	110.4307	109.6063
F_7-C_2-C_1	112.2997	**109.2**	109.201	112.26	107.4424	109.0626
Br_4-C_2-C_1	101.2127	**110.6259**	**110.626**	101.209	113.9482	110.3576
F_5-C_1-Br_3	112.4349	**109.4830**	109.483	112.483	110.4303	109.6092
F_5-C_1-F_6	106.3187	**108.8182**	108.818	106.302	106.8394	109.1160
F_5-C_1-C_2	112.2931	**109.2**	109.202	112.26	107.4430	109.0684
Br_3-C_1-F_6	112.4305	**109.4839**	**109.484**	112.484	110.4314	109.6069
Br_3-C_1-C_2	101.2107	**110.6249**	110.625	101.209	113.9474	110.3563
F_6-C_1-C_2	112.3016	**109.1999**	109.20	112.26	107.4415	109.0613
F_6-C_1-C_2-Br_4	-59.8738	-59.4399	-59.44	-59.843	-57.3226	-59.5435
F_6-C_1-C_2-F_7	-179.999	179.9993	179.99	180.000	179.9997	179.9993
F_6-C_1-C_2-F_8	60.2284	61.1194	61.1194	60.3136	60.3535	60.9198
Br_3-C_1-C_2-Br_4	-179.995	-179.999	-180.00	**180.00**	-180.00	-179.999
Br_3-C_1-C_2-F_7	59.8823	59.4393	59.4393	59.8447	57.3223	59.5430
Br_3-C_1-C_2-F_8	-59.8902	-59.4408	-59.44	-59.843	-57.3239	-59.5365
F_5-C_1-C_2-Br_6	59.8878	59.4398	59.4398	59.8447	57.3229	59.5365
F_5-C_1-C_2-F_7	-60.2376	-61.1211	-61.121	-60.310	-65.3548	-60.9207
F_5-C_1-C_2-F_8	179.9900	179.9991	179.999	180.000	179.9990	179.9999

The physical properties of Halon-2402 represented in figure 1. The negative electrostatic potential regions are diffuse on some atoms therefore there are incomplete distribution of electrostatic potential on the atoms and also in total charge. Also geometry optimization shapes at the two and three dimension for Halon-2402 shows the frontal orbital's distribution for high occupied orbital (**HOMO**) and low unoccupied orbital(**LUOM**) .

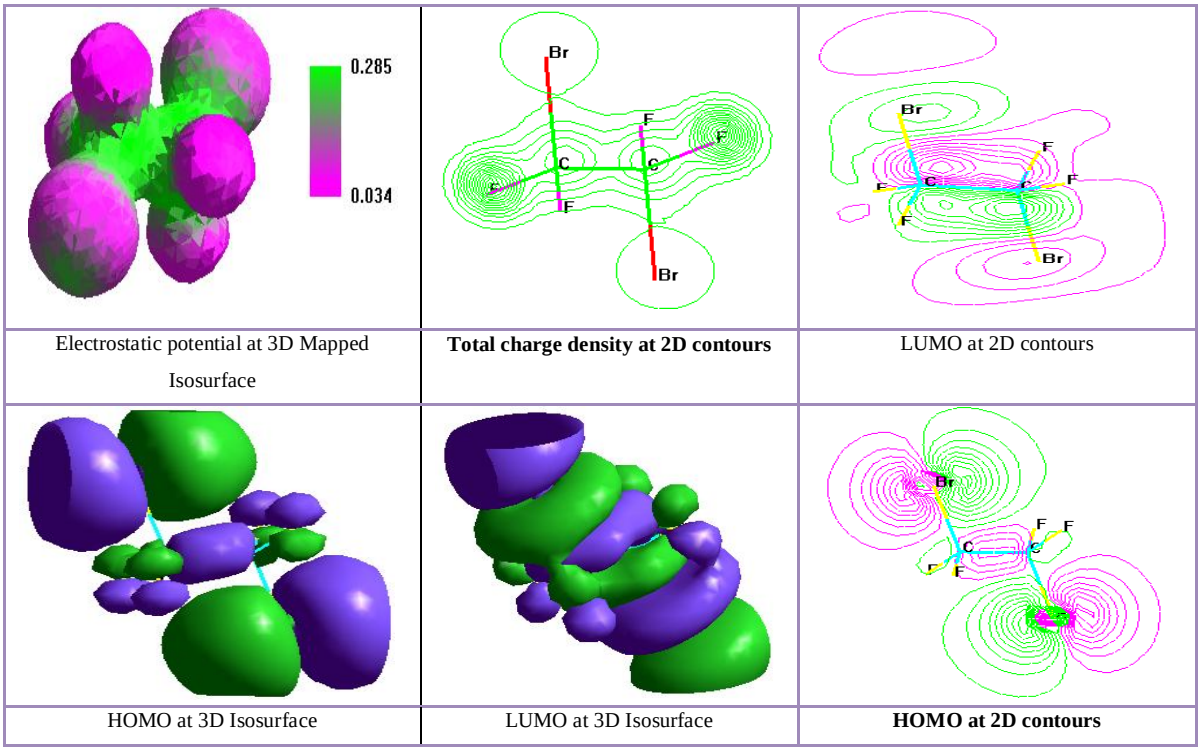

Electrostatic potential at 3D Mapped Isosurface	**Total charge density at 2D contours**	LUMO at 2D contours
HOMO at 3D Isosurface	LUMO at 3D Isosurface	**HOMO at 2D contours**

Figure 1. Geometry optimization of $C_2F_4Br_2$ calculated at B3LYP/3-21G+ //MP2/3-21G+(s,sp,6d) level of theory.

Figure .2 illustrates the stability of C-Br, C-F and C-C bond . The C-Br bond is more active toward the reactions than C-C and C-F bond. The equilibrium length C-Br bond at 1.93 Å (-3500260.5 kCal/mol) but at 3.4 Å (-3500204.06 kCal/mol) is broken down that's means the bond dissociation energy has to be 56.44 kCal/mol. The F-C bond is stable at 1.338 Å (-3490270.44 kCal/mol) and broken down at 2.93 Å (-3490130.55 kCal/mol) that's refer to the bond dissociation energy equal to 139.89 kCal/mol. The C-C bond have length stability equal to 1.546 Å (-3490320.33 kCal/mol) whereas 3.0 Å (-3490237.6 kCal/mol) therefore the bond dissociation energy is 82.73 kCal/mol. The values of energy C-Br and C-C bond equal to 66 and 83-85 kCal/mol respectively are calculated at 298.15 K over a large series of compounds[48] . This indication proof that the reaction of $C_2F_4Br_2$ molecule occurs through C-Br bond scission with high probability than C-C, C-F bond scission.

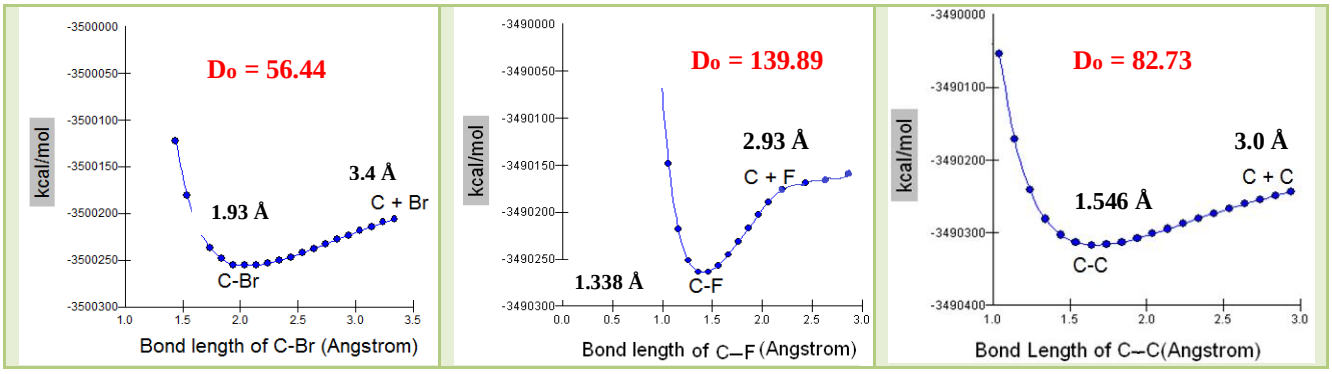

Figure 2. Potential energy stability curves of $C_2F_4Br_2$ molecule bonds length in calculated at B3LYP//3-21G+(s,sp,6d) level of theory .

The photolysis of Halon-2402 under atmospheric conditions will form the $^{\bullet}C_2F_4Br$ and $Br^{\bullet}$ radicals. The $^{\bullet}C_2F_4Br$ radical undergoes secondary decomposition depends upon the energy light of photolysis. The suggested reaction including $^{\bullet}C_2F_4Br$ radical formation, that's rapidly react with O_2 to form a peroxy radical ($C_2F_4BrO_2$). The radical $C_2F_4BrO_2$ will react primarily with NO to produce C_2F_4BrO and NO_2. The alkoxy radical C_2F_4BrO undergo C-C bond scission give up CF_2Br and CF_2O[15] . However, since the C-F bond is significantly stronger than the C-Cl bond. Little C–F bond cleavage channel would be expected for C_2F_4BrO radical dissociation[49] . The C-C bond breakage has been previously reported for C_2F_5O radicals .The $^{\bullet}CF_2Br$ undergo subsequent oxidation to yield CF_2O and $Br^{\bullet}$[50] . As a result, may be expected that both $Br^{\bullet}$ in the CF_2BrCF_2Br will be released as active bromine upon absorption of UV energy, that's leads to the ozone depletion process by conversion of O_3 into O_2 [51,52].

The reaction mechanism of ozone depletion is began by the reaction of $^{\bullet}C_2F_4Br$ with O_3 (instead of the reaction with O_2) to produce alkoxy radical C_2F_4BrO with E_b= 12.5 kCal/mol, k= 1.1×10^{7} and A= 1.6×10^{16} $mol^{-1}dm^3s^{-1}$ calculated by PM3CI(4x4) method . The reaction of ozone with $^{\bullet}C_2F_4Br$ is exothermic property (ΔH_r= -50.1 kCal/mol) , spontaneous (ΔG_r= -51.6 and ΔS_r= 0.050 kCal/mol) and the probability is increased with temperatures raised . The reaction of $^{\bullet}C_2F_4Br + O_2 \rightarrow C_2F_4BrO_2$ has activation energy equal to 14.3 kCal/mol, which is more than the reaction with ozone. Also the reaction with oxygen molecule is exothermic ΔH_r= -51.1 kCal/mol), and rate constant is k= 8.3×10^{2} and Arrhenius is A=2.5×10^{13} their lower than the reaction with ozone. But the only favorable for the reaction with O_2 is in the spontaneous state. The reaction with O_2 has ΔG_r= -75.7 kCal/mol and ΔS_r= 0.0824 kCal/mol that's more spontaneous in the view of thermodynamic aspect than with O_3, therefore, increasing of temperatures is more active with O_2 than O_3. At this point, the reaction with O_2 is more favorable in the thermodynamic aspect than kinetic aspect whereas the reaction with O_3 is more considering in the kinetic aspect than thermodynamic, but in any reaction, the kinetic considerations which is controlling and arbitrariness on the reaction[53,54] . Under this results, the dissociate of bromotetrafluoroethyle radical not requested to nitrogen oxide (NO) in order to convert peroxy radical ($C_2F_4BrO_2$) into alkoxy radical(C_2F_4BrO). The alkoxy radical undergoes dissociation C-C bond into $FCOF+^{\bullet}CF_2Br$ by 11.2 kCal/mol of energy barrier and 9.9×10^{4} s^{-1} of rate constant with A= 1.6×10^{13} s^{-1} due to the C-F bond is significantly stronger than the C-C bond[38] . This dissociation is exothermic (ΔH_r= -15.9) kCal/mol) and spontaneous reaction (ΔG_r= -30.2 and ΔS_r= 0.048 kCal/mol) in addition to that rising of temperatures will increased the spontaneously of reaction because of the ΔS is positive. The $^{\bullet}CF_2Br$ react with oxygen atom is exothermic and spontaneous in the view of thermodynamic aspect (ΔH_r= -114.1, ΔG_r= -104.4 and ΔS_r= -0.0352 kCal/mol) producing CF_2BrO by E_b= -2.5 kCal/mol and k = 5×10^{12} $mol^{-1}dm^3s^{-1}$ with A= 6.2×10^{10} $mol^{-1}dm^3s^{-1}$. But the reaction $^{\bullet}CF_2Br+O$ is barrierless reaction[55,56] and increasing the temperatures leading to decrease the rate and spontaneously reaction due to the Entropy is negative value. The CF_2BrO released of bromine radical to produced FCOF with low E_b= 0.48 kCal/mol and highest rate constant k = 6.7×10^{12} and A= 1.5×10^{13} s^{-1}. Releasing of bromine radical also is exothermic and spontaneous in the view of thermodynamic (ΔH_r= -9.7, ΔG_r= -18.62 ΔS_r= 0.0299 kCal/mol) and rise of temperatures is increasing for rate of reaction because of this step is broken bond. The two bromine radicals are reacts with ozone producing bromine oxide (BrO) and the last react with atomic oxygen to completely the depletion of ozone as shown in scheme- 1.

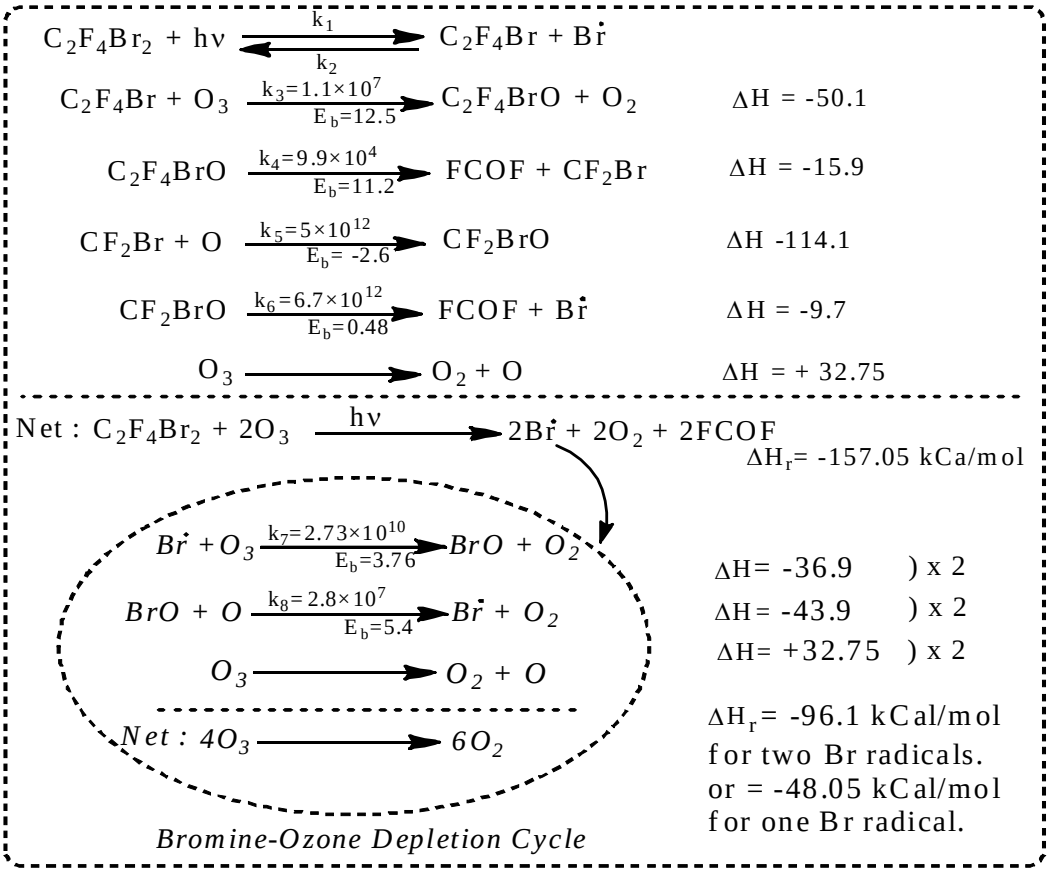

Scheme 1. Net equation of ozone depleting reaction mechanism when C_2F_4Br is dissociate calculated by PM3 CI(4x4).

The reaction of BrO+O is exothermic and spontaneous but increasing of temperatures is decline of the reaction probability (ΔH_r= -43.9 ΔG_r= -43.155 ΔS_r= -0.0025 kCal/mol). The BrO+O→$Br^{\bullet}$ + O_2 required to energy barrier is 5.4 kCal/mol with k= 2.8×10^7 and A= 2.5×10^{11} $mol^{-1}dm^3$ s^{-1}. Scheme 1 shows the dissociation of halon-2402 into 2FCOF + 2$Br^{\bullet}$ and ozone depletion cycle through bromine radical. The radical C_2F_4BrO not making the depletion ozone cycle as shown in scheme 1. The depletion of ozone resulted with two molecules that's needed to dissociate the Halon-2402 into 2$Br^{\bullet}$ + $2O_2$ + 2FCOF as a first step (ΔH_r= -157.05 kCal/mol), and four molecules from bromine of depletion cycle have ΔH_r= -96.1 kCal/mol for two $Br^{\bullet}$ radicals and ΔH_r= -48.05 kCal/mol for one Br radical (two ozone molecules is depletion at the same time). The final depletion in this state is four molecules in each two bromine radicals-ozone depletion cycle. According to the scheme 1 the rate of ozone depletion is depend on the rate of providing bromine radical in this state.

APPLICATIONS

The quantum calculation method suggest some reasonable mechanism for ozone depletion by Halon-2402 in stratospheric layer and estimation of the controlling condition that lead to consuming ozone layer.

CONCLUSION

- Depletion of ozone in stratospheric layer occurs by the photolysis reaction of Halon-2402 through C-Br bond, which needed 92.3 kcal/mol (309.95 nm) with highly probability than other bonds .
- The reaction of bromine radical with ozone is spontaneous and exothermic in gas phase has E_b= 0.044 kCal/mol with ΔH_r= - 34.5 kCal/mol and the rate constant is k= 3×10^{13} $mol^{-1}dm^3s^{-1}$ and A= 2.33×10^{13} at STP .
- The energy barrier of reaction $^{\bullet}C_2F_4Br+O_3$ equal to 11.9 kCal/mol, ΔH_r= -55.5 kCal/mol, k= 1.6×10^{7} $mol^{-1}dm^3s^{-1}$ and A= 2.7×10^{15} $mol^{-1}dm^3s^{-1}$ at STP .
- The depletion of ozone resulted by two moles of ozone through the photolysis of Halon-2402 into $2Br^{\bullet} + 2O_2 + 2FCOF$.

REFERENCES

[1] World Meteorological Organization (WMO), Scientific assessment of ozone depletion: 1991,WMO Global Ozone Res. and Monit. Proj. Rep. 25, **1992**.
[2] D. J. Chartrand, J. de Grandpré, and J. C. McConnell, Atmosphere-Ocean, 37, 4, 309–367, **1999**.
[3] A. C. Voukides, K. M. Konrad, and R. P. Johnson, J. Org. Chem., 74, 5, 2108-2113, **2009**.
[4] M. A. Mendes, L. A. B. Moraes, R. Sparrapan, M. N. Eberlin, R. Kostiainen, and T. Kotiaho,J. Am. Chem. Soc., 120, 31, 7869-7874, **1998**.
[5] S. Pekárek, Eur. Phys. J. D, 56, 91–98, **2010**.
[6] J. Skotnica, M. Gilbert , I. Weingart, and C. Wilhelm, Photosynthetica, 43, 3, 425-434, **2005**.
[7] J. Cerkovnik, B. Plesničar, J. Koller, and T. Tuttle, J. Org. Chem., 74, 1, 96–101, **2009**.
[8] A. L. Gomez, T. L. Lewis, S. A. Wilkinson, and S. A . Nizkorodov, Environ. Sci. Technol., 42, 10, 3582–3587, **2008**.
[9] J. C. Hansen, Y. Li and J. S. Francisco, and Z. Li, J. Phys. Chem. A, 103, 42, 8543-8546, **1999**.
[10] J .Struijs, A. V. Dijk, H. Slaper, H. J. Van Wijnen, G. J. M. Velders, G. Chaplin, and M. A. J. Huijbrets, Environ. Sci. Technol., 44, 1, 204–209, **2010**.
[11] W. S. McGivern, O. Sorkhabi, A. G. Suits, A. Derecskei-Kovacs, and S.W. North, J. Phys. Chem. A, 104, 45, **2000**.
[12] V. L. Orkin, F. Louis, R. E. Huie, and M. J. Kurylo, J. Phys. Chem. A, 106, 43, **2002**.
[13] P. J. Crutzen and F. Arnold, Nature, 324, 651-655, **1986**.
[14] P. Zou, W. S. McGivern, O. Sorkhabi, A. G. Suits, and S. W. North, J. Chem. Phys., 113, 17, 7149-7157, **2000**.
[15] A. Kalume, L. George, P. Z. El-Khoury, A. N. Tarnovsky, and S. A. Reid, J. Phys. Chem. A, 114, 36, 9919–9926, **2010**.
[16] I. K. Larin, T. I. Belyakova, N. A. Messineva, A. I. Spasskii, and E. M. Trofimova, Kinetics and Catalysis, 52, 4, 513–517, **2011**.
[17] B. R. J. Muhyedeen, European Journal of Scientific Research, 16, 4, 490-505, **2007**
[18] A. M. Thompson and R. W. Stewart, J. Geophys. Res., 96, 13, 89-108, **1991**
[19] D. G. Truhlar, Ann. Rev. Phys. Chem, 1, 35, 159-189, **1984**.

[20] HyperChem ^{TM} 8.0.9. for windows molecular modeling system, Hypercupe, Inc., **2011**.
[21] S. Grimme, Journal of Chemical Physics, 124, 3, 034108 (1-16), **2006**.
[22] U. Zimmerli, M. Parrinello, and P. Koumoutsakos, Journal of Chemical Physics, 120, 6, 2693–2699, **2004**.
[23] S. Grimme, Journal of Computational Chemistry, 25, 12, 1463–1473, **2004**.
[24] H. Dorsett, and A. White, DSTO-GD-0253, **2000**.
[25] F. Jensen, "Introduction to Computational Chemistry", 2nd Ed. , John Wiley & Sons, Ltd. , **2007**.
[26] J. S. Binkley, J. A. Pople, and W. J. Hehre, J. Am. Chem. Soc., 102, 3, 939-947, **1980**.
[27] M. S. Gordon, J. S. Binkley, J. A. Pople, W. J. Pietro, and W. J. Hehre, J. Am. Chem. Soc., 104, 2797-2803, **1982**.
[28] W. J. Pietro, M. M. Francl, W. J. Hehre, D. J. Defrees, J. A. Pople, and J. S. Binkley, J. Am. Chem. Soc., 104, 5039-5048, **1982**.
[29] M. He, Y. Sun, H. Cao, D. Han, and J. Hu, Struct Chem, DOI 10.1007/s11224-011-9866-0, **2011**.
[30] K. Brudnik , J. T. Jodkowski , D. Sarzyński, and A. Nowek, J. Mol. Model, 17, 2395–2409, **2011**.
[31] A. Ciancetta, C. Coletti, A. Marrone, and N. Re, Theor. Chem. Acc., 129, 757–769, **2011**.
[32] M. Vahedpour, and F. Zolfaghari, Struct Chem, DOI 10.1007/s11224-011-9823-y, **2011**.
[33] A. Hamza, Á . VibÓK, G. J. Halász, and I. Mayer, Journal of Molecular Structure: Theochem, 501–502, 427–434, **2000**.
[34] B. N. Plakhutin, and K. D. Sen, "Reviews of Modern Quantum Chemistry", 1st Ed., Word Scientific, **2002**.
[35] K. R. Glaesemann, and M. W. Schmidt, The Journal of Physical Chemistry A, 114, 33, 8772–8777, **2010**.
[36] I. A. Adejoro, and E. Ekeh, E-Journal of Chemistry, 7, 1, 271-274, **2010**.
[37] I. Sheikhshoaie, and S. Saeednia, The Arabian Journal for Science and Engineering, 35, 1A, 53-60, **2010**.
[38] H. J. Singh, B. K. Mishra, and N. K. Gour, Bull. Korean Chem. Soc., 30, 12, 2973-2978, **2009**.
[39] H. Liu, J. Tao, J. Xu, Z. Chen, and X. Luo, 256, 20, 5939-5945, **2010**.
[40] G. Maroulisa, J. Chem. Phys., 111, 15, 6846-6849, **1999**.
[41] Z. F. Xu, and M. C. Lin, J. Phys. Chem. A, 114, 43, 11477-11482, **2010**.
[42] Hypercup, Inc., Hyperchem Computational Chemistry, Practical Guide, Hypercup, Inc., USA, **2002**.
[43] A. J. Hameed, Journal of Molecular Structure: Thochem, 764, 195-199, **2006**.
[44] A. J. Hameed, Journal of Molecular Structure: Thochem, 725, 97-101, **2005**.
[45] A. A. Drea, S. N. Naman, and B. R. J. Muhyedeen, NJC, 44, 539-560, **2011**.
[46] A. A. Drea, NGC, 39, 481-498, **2009**.
[47] M. Ibrahim, H. El-Haes, A. J. Hameed, and A. F. Jalbout, J. Comput. Theor. Nanosci., 5, 11, 1-5, **2008**.
[48] R. A. Moss, M. S. Platz, and Jr. M. Jones, "Reactive Intermediate Chemistry", John Wiley & Sons, Inc., Hoboken, New Jersey, **2004**.
[49] H. Ihee, J. Cao, and A. H. Zewail, Chem. Phys. Lett., 281, 10-19, **1997**.
[50] H. Ihee, J. Kua, W. A. Goddard, and A. H. Zewail, J. Phys. Chem. A, 105, 14, 3623-3632, **2001**.

[51] J. Fossey, D. Lefort, J. Sorba,"Free Radicals in Organic Chemistry", John Wiley & Sons, New York, **1995**.
[52] M. B. Smith, and J. March," March's Advanced Organic Chemistry: Reactions, Mechanisms, and Structure", 6th Edition, John Wiley & Sons, Inc, **2007**.
[53] D. Y. Hwang, and A. M. Mebel, J. Chem. Phys., 109, 24,10847-10851, **1998**.
[54] Z. Li, J. Phys. Chem. A, 103, 9, 1206-1213, **1999**.
[55] À. González-Lafont, J. M. Lluch, A. Varela-Álvarez, and J. A. Sordo, J. Phys. Chem. B, , 112, 2, 328–335, **2008**.
[56] D. C. Young, "Computational Chemistry: A Practical Guide for Applying Techniques to Real-World Problems", New York, John Wiley & Sons, Inc, **2001**.